

Identification of key genes related to heart failure by analysis of expression profiles

Che Wang, Qingmin Li, Honghui Yang, Chuanyu Gao, Qiubo Du, Caili Zhang, Lijie Zhu, Qingman Li

Department of Cardiology, Henan Provincial People's Hospital, Fuwai Central China Cardiovascular Hospital, People's Hospital of Zhengzhou University, Zhengzhou, Henan, China

Submitted: 21 June 2019; **Accepted:** 28 November 2019

Online publication: 10 March 2021

Arch Med Sci 2024; 20 (2): 517–527

DOI: <https://doi.org/10.5114/aoms/114896>

Copyright © 2021 Termedia & Banach

Abstract

Introduction: To elucidate the candidate biomarkers involved in the pathogenesis process of heart failure (HF) via analysis of differentially expressed genes (DEGs) of the dataset from the Gene Expression Omnibus (GEO).

Material and methods: The GSE76701 gene expression profiles regarding the HF and control subjects were respectively analysed. Briefly, DEGs were firstly identified and subjected to Cytoscape plug-in ClueGO + CluePedia and Kyoto Encyclopedia of Genes and Genomes (KEGG) enrichment analyses. A protein-protein interaction (PPI) network was then built to analyse the interaction between DEGs, followed by the construction of an interaction network by combining with hub genes with the targeted miRNA genes of DEGs to identify the key molecules of HF. In addition, potential drugs targeting key DEGs were sought using the drug-gene interaction database (DGIdb), and a drug-mRNA-miRNA interaction network was also constructed.

Results: A total of 489 DEGs were verified between HF and control, which mainly enriched in type I interferon and leukocyte migration according to molecular function. Significantly increased levels of GAPDH, GALM1, MMP9, CCL5, and GNAL2 were found in the HF setting and were identified as the hub genes based on the PPI network. Furthermore, according to the drug-mRNA-miRNA network, FCGR2B, CCND1, and NF- κ b, as well as corresponding miRNA-605-5p, miRNA-147a, and miRNA-671-5p were identified as the drug targets of HF.

Conclusions: The hub genes GAPDH, GALM1, MMP9, CCL5, and GNAL2 were significantly increased in HF. miRNA-605-5p, miRNA-147a, and miRNA-671-5p were predicted as the drug target-interacted gene-miRNA of HF.

Key words: heart failure, differentially expressed gene, enrichment analysis, PPI network, drug-mRNA-miRNA network.

Corresponding authors:

Che Wang
Department of Cardiology
Henan Provincial People's Hospital
Fuwai Central China
Cardiovascular Hospital
People's Hospital
of Zhengzhou University
No. 7 Weiwu Road
Zhengzhou, Henan,
450003, China
Phone: +86-15937172693
E-mail: wangche10@163.com

Qingmin Li
Department of Cardiology
Henan Provincial Peoples
Hospital
Fuwai Central China
Cardiovascular Hospital
Peoples Hospital of
Zhengzhou University
No. 7 Weiwu Road
Zhengzhou, Henan
450003, China
E-mail: lqm1973@163.com

Introduction

Heart failure (HF), caused by the insufficient supply of oxygenated blood to the heart and thereby resulting in hypertrophied heart without normal functions, is a major cause of death in the world, especially in an aging population [1]. Multiple complications such as myocardial infarction [2] are presented in the setting of HF, with the number of affected subjects reaching more than 40 million globally [3]. Many novel drugs and new treatment methods for HF have been studied and applied in clinical treatment [4, 5]. Early detection of HF is critical for the management of this debilitating disease [6], but the involved molecular mechanisms

are not completely understood and biomarkers for early diagnosis remain controversial.

In 2014, Oka *et al.* [7] elaborated on the pathology and molecular mechanisms of HF: angiogenesis increased the endothelium-derived NO release, resulting in degradation of regulator of G-protein signalling 4 (RGS4), and activated the PI3K γ /Akt/mTORC1 (phosphatidylinositol 3-kinase/Akt/mammalian target of rapamycin C1) pathway, which finally induced myocardial hypertrophy. Then, hypertrophic responses inversely induced myocardial angiogenesis by overexpressed vascular endothelial growth factors (VEGFs) and by inhibition of the PI3K γ /Akt/mTORC1 pathway. Also, there is obvious accumulation of p53 in hypertrophied myocardium of HF [7–9]. Biochemical markers that have been validated and are usually used in diagnosis and prognosis of HF mainly contain B-type natriuretic peptide and N-terminal pro-B-type natriuretic peptide [10–12]. In addition, single nucleotide polymorphisms (SNPs) have been reported to be significantly correlated with HF [13, 14]. Despite intensive study in HF pathogenesis and therapies, the incidence and recurrence rate remain high, resulting in physical suffering and economic costs [15].

In the present study, using the microarray GSE76701 datasets, differentially expressed genes (DEGs) were firstly identified. Then, via construction of the enrichment analysis, protein-protein interaction (PPI) network, and drug-mRNA-miRNA interaction network, the analysis of mRNA profiles allowed us to better understand the effect of DEGs and related miRNA on the potential pathogenesis of HF.

Material and methods

Data sources and preprocessing

Gene profiles of GSE76701 [16] were obtained from the National Centre of Biotechnology Information (NCBI) Gene Expression Omnibus database (GEO). GSE76701 was processed on Affymetrix Human Genome U133 Plus 2.0 Array (GPL570). GSE76701 contained 4 HF and 4 normal controls, and the mRNA was isolated from left ventricular tissue for microarray analysis.

For preprocessing, text files (.txt) from GSE76701 were collected, and probe IDs were converted to gene symbols according to the annotation file. When multiple probes matched the same gene symbol, the average value of the probes was taken as the gene expression level. Unmatched probes were excluded from this study.

Screening of differentially expressed genes

For DEGs between HF and control, the *p*-value and logarithmic fold change (\log_2FC) were calculated using a freely available limma package (<http://bioconductor.org/packages/release/bioc/>

<http://limma.html>, version 3.26.9) [17]. DEGs were determined by the threshold of *p*-value < 0.05 and $|\log_2FC| > 0.585$.

Bidirectional hierarchical clustering analysis of differentially expressed genes

Hierarchical clustering is usually used to discover the closest associations that exist between gene profiles and samples [18]. Generally, even in the same tissue, there are significant differences in gene profiles between disease states and normal. To analyse whether these DEGs would segregate the samples into 2 distinct clusters, bidirectional hierarchical clustering was conducted by ‘pheatmap’ package (version 1.0.8) using Euclidean distance function [19].

Enrichment analyses of differentially expressed genes

Based on the Cytoscape plug-in ClueGO + CluePedia [PMID: 19237447], the target protein was analysed for GO function [PMID: 10802651], and the GO biological process with significance threshold was set to $P_{\text{adjust}} \leq 0.01$ was selected. Then, Cytoscape was used for a functional network map construction of the target protein.

Pathway enrichment analysis was applied by clusterProfiler in R package (version 3.2.11). In this study, Fisher’s exact test was adopted to evaluate important pathways based on the Kyoto Encyclopedia of Genes and Genomes (KEGG) [20, 21]. Pathways with a *p*-value less than 0.01 were determined to be statistically significant.

Protein-protein interaction network and module analysis

In order to analyse the interaction between DEG-related proteins, the Search Tool for the Retrieval of Interacting Genes (STRING) database (version 10.0, <http://www.string-db.org/>) was used to obtain the PPI relationships [22]. The relationships whose required confidence (combined score) was greater than 0.4 were selected to build the network using Cytoscape software. Topological features such as degree centrality (DC), betweenness centrality (BC), and closeness centrality (CC) were further analysed using a CytoNCA plugin (version 2.1.6) [23]. According to the score ranking of nodes, important proteins (hub protein) were identified [24]. Taking into account the fact that the resulting network was too large, the MCODE plugin (version 1.4.1) was applied to analyse the subnetwork of the PPI network [25]. Subnetworks with scores higher than 5 based on the default threshold (Degree Cutoff: 2, Node Score Cutoff: 0.2, K-Core: 2, Max. Depth: 100) were retained for further analysis. Genes with the most links with other genes were considered to be the

hub genes [26], while we used a cut-off degree value range of 25–30, and combined top 5–10 ranking was used as the criteria to identify these hub genes according to previous description [27].

Target miRNA of the differentially expressed genes

The miRWalk 2.0 database was applied to acquire all the target miRNAs of DEGs [28]. Then, 7 databases (miRWalk, RNA22, miRanda, Targets-can, miRDB, miRMap, and miRBridge) were added to assist in predicting interactions between DEGs and miRNAs. According to the miRWalk 2.0 database, miRNAs that appeared in at least 7 databases were chosen as the target miRNAs. Finally, the intersection of DEGs and related miRNA was taken to obtain the miRNA-mRNA regulatory relationship pairs. Based on the DEG and related miRNA, enrichment analysis was performed by clusterProfiler package.

Drug-gene interaction prediction

Potential drugs targeting key DEGs confirmed by network module analysis were searched using the drug-gene interaction database (DGIdb, <http://dgidb.genome.wustl.edu/>) [29] with the following values: Preset Filter: FDA Approved + Antineoplastic; Advanced Filters: Source Databases: FDA and Drug-Bank; Gene categories: All; Interaction Types: All. All the drug-gene relationship pairs related to the pre-

dicted gene, and the regulatory miRNAs were employed to construct an miRNA-gene-drug regulatory network map using Cytoscape network construction software (version: 3.2.0, <http://www.cytoscape.org/>).

Results

Identification of differentially expressed genes

After normalising the raw data and transforming the probe ID to gene symbol, 21,655 mRNAs were obtained for GSE76701. DEGs were determined with the threshold of p -value and $|\log_2FC|$. There were 489 DEGs in GSE76701, including 271 up- and 218 down-regulated genes. Volcano plots show the distribution of the 489 genes in Figure 1 A.

Bidirectional hierarchical clustering analysis

Based on the DEGs, bidirectional hierarchical clustering analysis was conducted. As shown in cluster heat maps (Figure 1 B), there are distinctive expressed change patterns in the HF and normal. DEGs further segregated the samples into 2 distinct groups.

Functional enrichment analysis of differentially expressed genes

GO function enrichment analysis was performed to elucidate the functions of the differential mRNA.

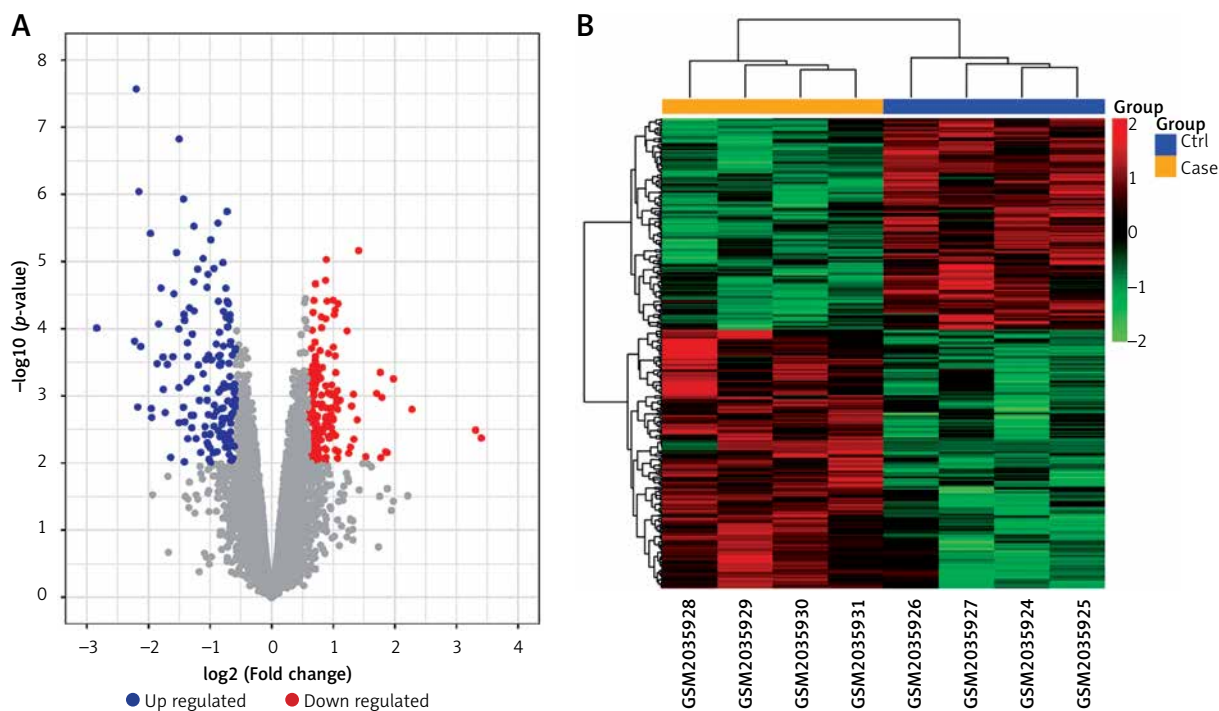


Figure 1. Volcano plot (A) and Heatmap (B) of DEGs between control and heart failure (HF) samples. **A** – exhibit the DEGs. X-axis: \log_2FC ; Y-axis: the log-transformed p -values. A total of 489 differential mRNAs were divided into 271 up(red)- and 218 down(blue) regulated mRNAs in GSE76701. **B** – column on the top of the heatmap represents, respectively, the HF group (yellow) and the control group (blue). Upregulated and downregulated genes were respectively marked in green and red

The 271 up-regulated mRNAs were subjected to ClueGO analysis, and a total of 25 GO terms were enriched (Figure 2 A), while the pie graph shows 7 categories of functional enrichment according to the Kappa coefficient (Figure 2 B).

The GO functional network diagram of upregulated genes is also shown (Figure 2 C). The 85 genes of the functional network were co-enriched in 25 significant GO functional terms. The seven main function terms include cytokine stimulated response, cell response to interferon γ , response to oxygen levels, growth factor response, vascular system development regulation, positive regulation of phosphoprotein phosphatase activity, and metal ion transport regulation.

The 218 downregulated mRNAs were also subjected to clueGO analysis, and a total of 3 GO terms were enriched (Figure 3 A), while the pie graph shows 2 categories of functional enrichment according to the Kappa coefficient (Figure 3 B).

The GO functional network diagram of up-regulated genes is also shown (Figure 3 C). The 15 genes of the functional network were co-enriched in 3 significant GO functional terms. The two main function terms include the regulation of inflammatory response and the positive regulation of inflammatory response.

KEGG pathway enrichment analysis was also performed (Figure 4), and a total of 41 significant pathways were enriched, including 30 upregulated gene-enriched pathways and 11 downregulated gene-enriched pathways. The upregulated genes were mainly enriched in human cytomegalovirus infection, viral myocarditis, and Kaposi's sarcoma-associated herpesvirus infection. The down-regulated genes were mainly enriched in pathways such as complement and coagulation cascade, *Staphylococcus aureus* infection, and drug metabolism-cytochrome P450.

Protein-protein interaction network and module analysis of differentially expressed genes

In order to analyse the interaction between genes, STRING software was applied to establish the PPI network. A total of 997 interaction pairs and 306 nodes were contained in the PPI network, with the threshold of combined score > 0.4 . Based on the topological properties, the top 5 genes with the degrees higher than 28 were chosen as the hub genes, namely glyceraldehyde-3-phosphate dehydrogenase (*GAPDH*), calmodulin 1 (*CALM1*), matrix metalloproteinase 9 (*MMP9*), chemokine (C-C motif) ligand 5 (*CCL5*), and guanine nucleotide-binding protein G(i) α -2 (*GNAI2*). After analysing the PPI network by MCODE plugin, a total of 16 subnetworks were obtained. Figure 5 shows the top 4 subnetworks with scores greater than 5.

Cluster 1 covered 25 genes and 146 relationship pairs with the highest score of 12.167, including 2 hub genes: *GNAI2* and *CCL5*. Cluster 2, with the score of 7.571, also contained 2 hub genes: *MMP9* and *GAPDH*. *CALM1* was found in cluster 4 and showed the highest association with others. There was no hub gene in cluster 3. All the hub genes were upregulated compared to normal samples.

Target miRNA of the differentially expressed genes

The miRWalk 2.0 database was used to predict the target miRNA of DEGs; as a result, 15 relationship pairs appeared in at least 7 databases. After removing the repeats, 15 miRNAs and 9 mRNAs were obtained. Next, these 9 mRNA-involved pathways in the above analysis were screened out as the regulation pathway for the 15 miRNAs. A total of 27 pathways were screened out (Table I).

Drug-gene interaction prediction analysis

For the drug-gene association prediction analysis, 9 drugs and 3 related genes were obtained. Moreover, 3 miRNAs of these 3 genes were also included, and the regulatory relationship network of drug-mRNA-miRNA was constructed (Figure 6). According to the drug-mRNA-miRNA network, *FCGR2B*, *CCND1*, and *NF- κ B*, as well as corresponding miRNA-605-5p, miRNA-147a, and miRNA-671-5p, were identified as the drug targets of HF.

Discussion

Due to its high morbidity and mortality, HF has always been a hotspot of medical attention. Biochemical markers that have been validated and are usually used in the diagnosis and prognosis of HF mainly contained B-type natriuretic peptide and N-terminal pro-B-type natriuretic peptide [10]. Despite intensive study in HF pathogenesis and therapies, the incidence and recurrence rate remain high, resulting in physical suffering and economic costs [15]. Therefore, a lot of evidence indicates that novel gene and molecules play an important role in the cardiovascular system and provide a new perspective into the pathophysiology as well as pharmacological targets of HF. Analysis of DEG of HF has been widely used to reveal the potential pathogenesis, which also enabled the extraction of targets for therapeutic strategies [30, 31]. Furthermore, Hu *et al.* identified key proteins and lncRNAs in hypertrophic cardiomyopathy based on integrated network analysis [32]. In the present study, gene expression profiles were analysed by means of bioinformatics, including function and pathway enrichment, PPI, and drug-mRNA-miRNA interaction networks. According to the results of mRNA profiles, a total of 489

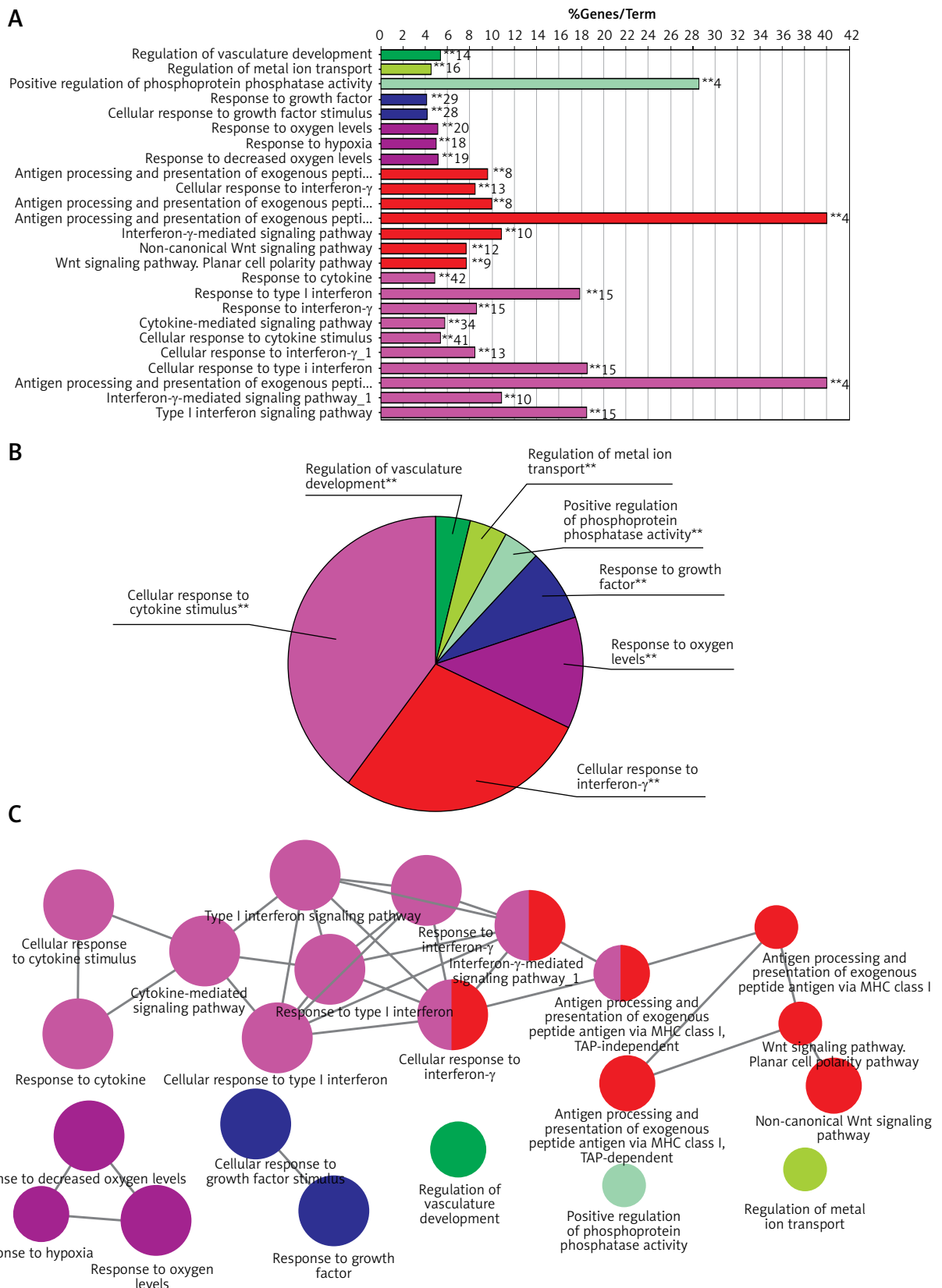


Figure 2. Functional enrichment analysis of upregulated DEGs. **A** – X-axis represents the percentage of enriched genes among the functional term-related genes, and the Y-axis gives the name of the GO term and is consistent with the pie graph. The number on the right side of the bar shows the number of related genes enriched in the relevant GO function term in the list of uploaded genes. * represents a p -value between 0.01 and 0.05, while ** represents $p < 0.01$. **B** – Functionally enriched pie graph, which represents the ratio of 3 groups of GO function. **C** – ClueGO Functional Network Diagram of upregulated DEGs. The dot is a GO function term. The larger the p -value, the larger the size of the dot. The 2-point connection represents the correlation between the functions, and the larger the kappa coefficient, the thicker the line. Multicolour dots represent multiple GO functions

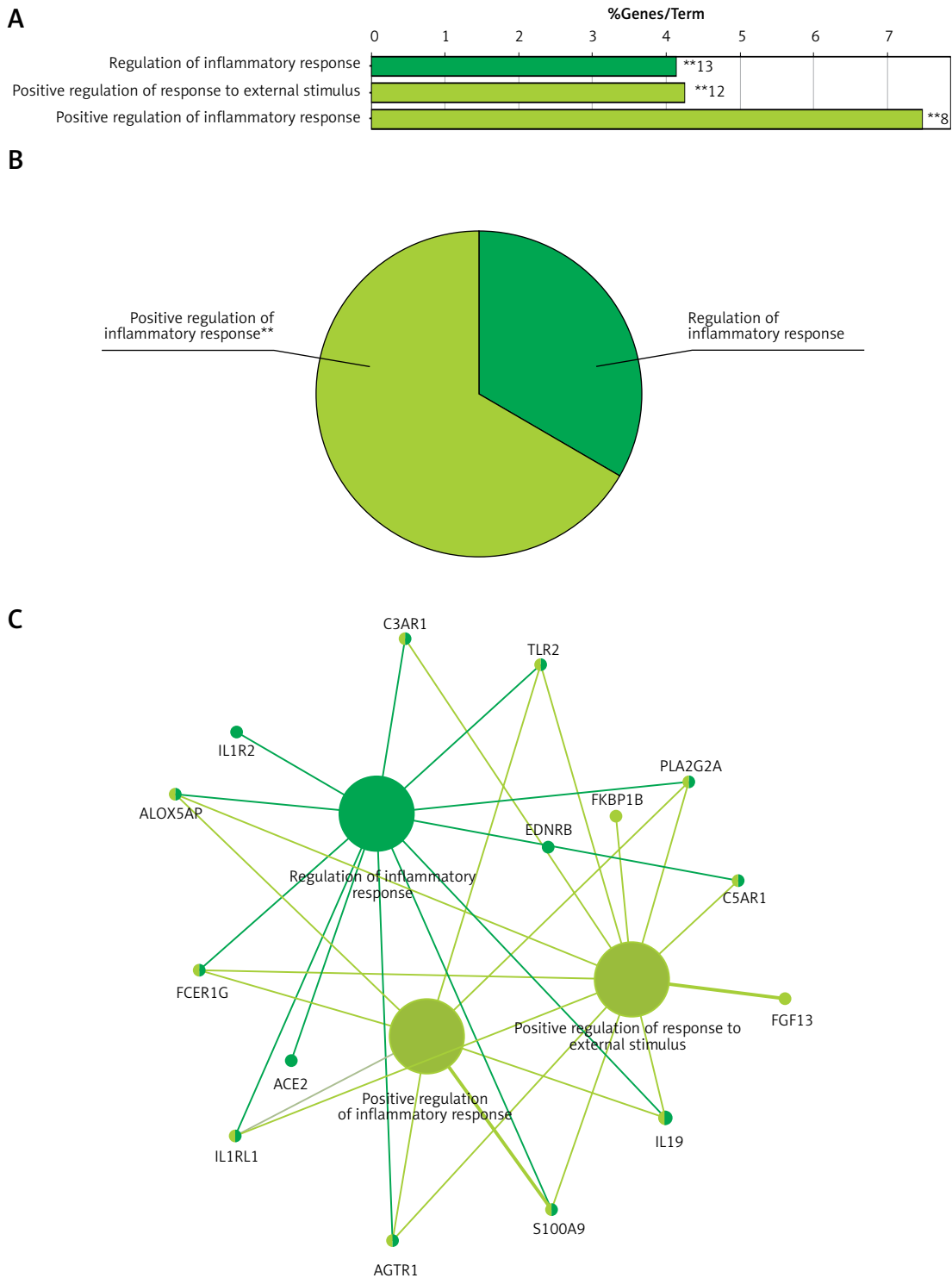


Figure 3. Functional enrichment analysis of downregulated DEGs from GSE76701. **A** – Downregulated DEGs between HF and control were functionally classified via GO analysis. X-axis represents the percentage of enriched genes among the functional term-related genes, and the Y-axis gives the name of the GO term and is consistent with the pie graph. The number on the right side of the bar is the number of related genes enriched in the relevant GO function term in the list of uploaded genes. * represents a p -value between 0.01 and 0.05, while ** represents $p < 0.01$. **B** – Functionally enriched pie graph, which represents the ratio of 2 groups of GO function. **C** – ClueGO Functional Network Diagram of downregulated genes. Red label corresponding to the dot is the enriched differential gene. The dot is a GO function term. The larger the p -value, the larger the size of the dot. The 2-point connection represents the correlation between the functions, and the larger the κ coefficient, the thicker the line. Multicolour dots represent multiple GO functions

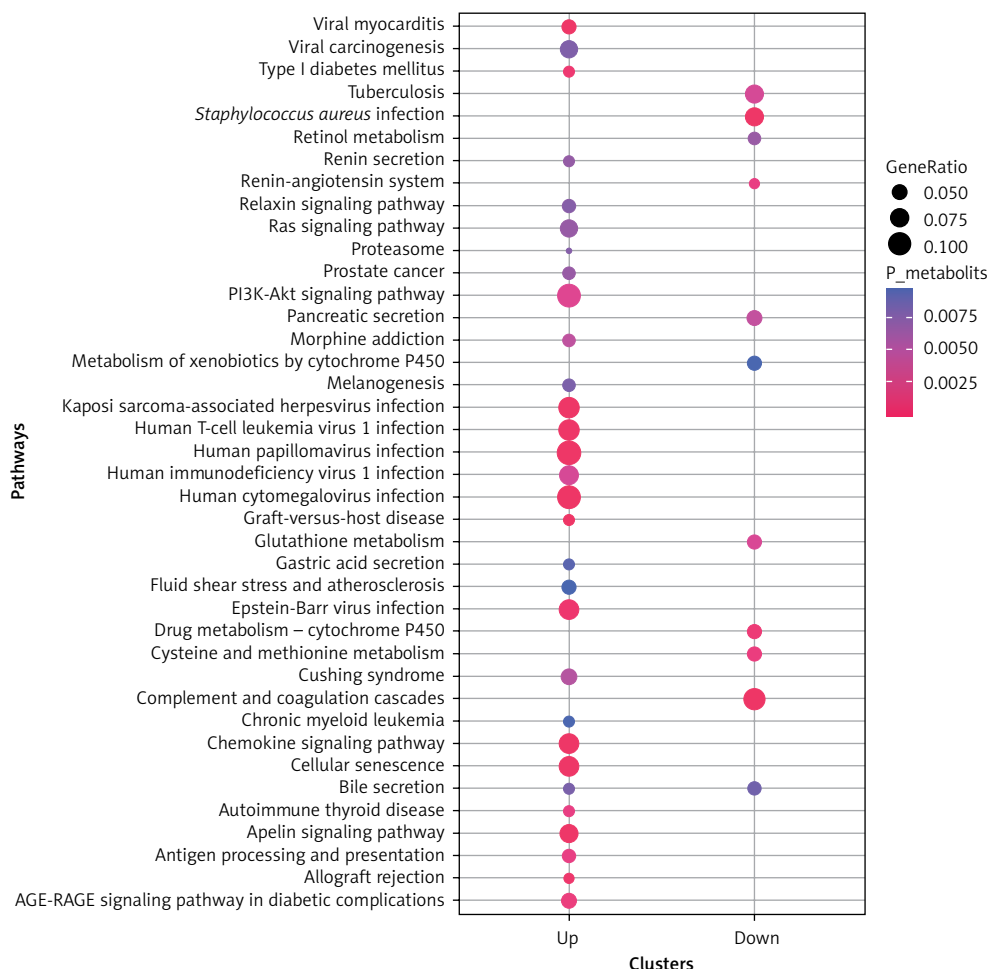


Figure 4. The bubble diagrams of Kyoto Encyclopedia of Genes and Genomes (KEGG) pathway on differentially expressed mRNA. X-axis represents upregulated or downregulated enriched gene entries. Y-axis represents KEGG pathways. The size of dots represents the ratio of the number of enriched genes to the total number of uploaded genes, and the larger the ratio, the larger the dot. The colour gradation from blue to red suggests that the *p*-values becomes smaller, and the significance is higher

DEGs were verified between HF and control, which mainly enriched in type I interferon and leukocyte migration according to molecular function. Significantly increased levels of GAPDH, GALM1, MMP9, CCL5, and GNAL2 were found in the HF setting and were identified as the hub genes based on the PPI network. Furthermore, according to the drug-mRNA-miRNA network, FCGR2B, CCND1, and NF- κ b, as well as corresponding miRNA-605-5p, miRNA-147a, and miRNA-671-5p, were identified as the drug targets of HF.

Matrix metalloproteinase 9 (MMP-9) is an enzyme that belongs to the zinc-metalloproteinase family, taking part in the degradation of the extracellular matrix. It is known that MMPs are closely related to left ventricular function after myocardial infarction, and the activity of MMPs tends to cause endocardial endothelial-myocyte disconnection, thereby resulting in myocardial contractile dysfunction [33]. In MMP-9 knockout HF mice, attenuated myocardial contractile dys-

function was observed [34]. Moreover, by monitoring of the plasma levels of MMPs, individuals with high levels of MMP-9 expression appeared to have a major risk of developing congestive HF [35]. Furthermore, reduced cardiac MMP-9 level was found in ischaemic HF mice (left coronary artery permanent ligation) treated with a neutralising CCL5 monoclonal antibody, and a shrink infarct size was confirmed [36]. Consistent with the above reports, herein we found that the MMP9 and CCL5 were significantly upregulated compare with controls.

Furthermore, in recently published study, Wang *et al.* [37] analysed the gene expression profile GSE57338 involving 117 ischaemic cardiomyopathic HF and 136 control samples with various bioinformatics approaches. The DEGs were categorised by several relationships, such as interferon regulatory factor 1 (IRF1)-CCL5, which were revealed in the transcription factor microRNA target gene regulatory network. Wang *et al.* also stated that CCL5 may participate in HF progression via protein

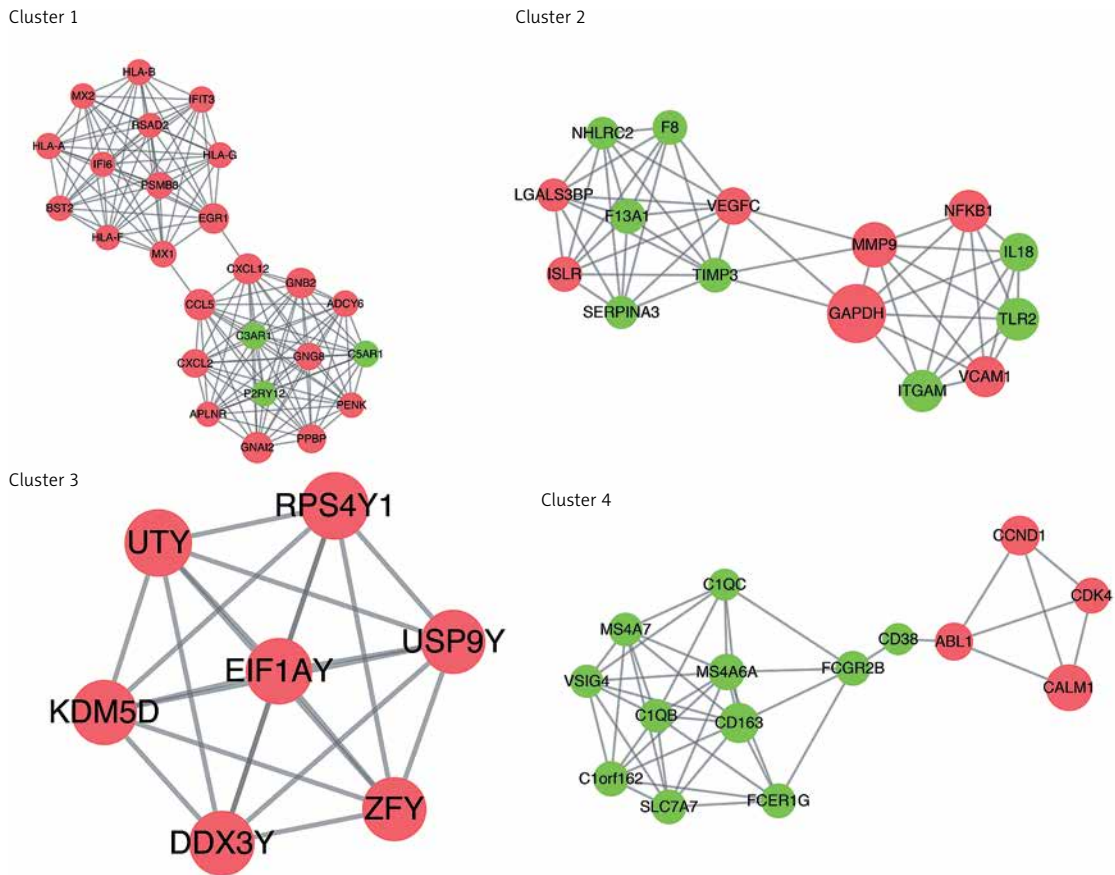


Figure 5. Sub-PPI network constructed from differential mRNA from GSE76701. Cluster 1 contains 25 genes and 146 edges with a score of 12.167; cluster 2 contains 15 genes and 53 edges with a score of 7.571; cluster 3 contains 7 genes and 21 edges with a score of 7; cluster 4 contains 15 genes and 43 edges with a score of 6.143. Pink represents upregulation, green represents downregulation. The size of the circle represents the degree of association of the node genes. The larger the dot, the greater the degree of genetic association

ubiquitination and CCL5 may participate in HF via IRF1-CCL5 interaction. Herein, we also found that CCL5 might be implicated in the progression of HF, which is consistent with the study by Wang *et al.*

In HF-related literature, Gapdh was the most frequently used reference gene in quantification of gene expression [38, 39]. Based on the geNorm and Normfinder algorithms, the most stable reference genes between HF and control tissues of mouse, rat, and human were Rpl32 and Polr2a, rather than Gapdh [40]. In our study, there was a significant difference in the expression of Gapdh between HF and the normal group. Ca²⁺ is arguably the most important second messenger in cardiac muscle, and the changes in the intracellular Ca²⁺ concentration have both acute and chronic effects on cardiac function. Ca²⁺/calmodulin-dependent protein plays an important role in cardiac hypertrophy and HF [41]. Many mutation sites of CALM1 have been reported to be associated with HF. For example, chronic heart failure (CHF) in patients carrying the CC genotype of rs3814843 on the CALM1 gene had greater risk of sudden cardi-

ac death and all cause death [42]. A mutation in CALM1 (p.Phe90Leu) encoding calmodulin causes sudden cardiac death in childhood and adolescence [43]. However, the change in the expression of CALM1 has not been specifically reported.

Moreover, miRNAs could regulate gene expression at the post-transcriptional level [44]. Functional miRNA studies revealed that many miRNAs had a great impact on the pathological mechanism related to HF, such as vascular remodelling, cardiac fibrosis, and hypertrophy [45]. Based on the global miRNA profile of ventricles of HF mice, decreased expression of miR-1 and miR-133a induced upregulation of target genes, resulting in cardiac hypertrophy. Also, a large number of miRNAs appeared to have an upregulated pattern in different stages of HF [46]. By analysing the circulating miRNAs of 39 normal control, 30 HF, and 20 dyspnoeic patients, miR-423-5p was especially accumulated in HF and determined as a strong diagnostic biomarker of HF, with an area under the receiver operator characteristics (ROC) curve of 0.91 [47]. Actually, the relationships of differentially expressed miRNA and aetiolo-

Table I. Targeted miRNAs were mainly enriched in 27 Kyoto Encyclopedia of Genes and Genomes pathways

No.	Cluster	ID	Description	Gene-ratio	BgRatio	P-value	p-adjust	q-value	Count
1	Up	hsa05163	Human cytomegalovirus infection	0.104478	225/7847	2.74E-05	2.74E-05	0.003388	14
2	Up	hsa05416	Viral myocarditis	0.052239	59/7847	5.89E-05	5.89E-05	0.003388	7
3	Up	hsa05167	Kaposi sarcoma-associated herpesvirus infection	0.089552	186/7847	7.46E-05	7.46E-05	0.003388	12
4	Up	hsa05166	Human T-cell leukemia virus 1 infection	0.097015	219/7847	8.74E-05	8.74E-05	0.003388	13
5	Up	hsa04062	Chemokine signaling pathway	0.089552	190/7847	9.16E-05	9.16E-05	0.003388	12
6	Up	hsa04371	Apelin signaling pathway	0.074627	137/7847	0.00011	0.00011	0.003388	10
7	Up	hsa05165	Human papillomavirus infection	0.119403	330/7847	0.000148	0.000148	0.003906	16
8	Up	hsa04218	Cellular senescence	0.074627	160/7847	0.00039	0.00039	0.008854	10
11	Up	hsa05169	Epstein-Barr virus infection	0.08209	201/7847	0.000622	0.000622	0.010472	11
13	Up	hsa04933	AGE-RAGE signaling pathway in diabetic complications	0.052239	100/7847	0.001549	0.001549	0.022082	7
16	Up	hsa04151	PI3K-Akt signaling pathway	0.104478	354/7847	0.002791	0.002791	0.032315	14
17	Up	hsa05170	Human immunodeficiency virus 1 infection	0.074627	212/7847	0.003309	0.003309	0.036059	10
18	Up	hsa05032	Morphine addiction	0.044776	91/7847	0.004511	0.004511	0.046428	6
19	Up	hsa04934	Cushing syndrome	0.059701	155/7847	0.004935	0.004935	0.04812	8
20	Up	hsa05215	Prostate cancer	0.044776	97/7847	0.006156	0.006156	0.051841	6
21	Up	hsa04014	Ras signaling pathway	0.074627	232/7847	0.006233	0.006233	0.051841	10
22	Up	hsa04924	Renin secretion	0.037313	69/7847	0.00632	0.00632	0.051841	5
23	Up	hsa04926	Relaxin signaling pathway	0.052239	130/7847	0.006712	0.006712	0.051841	7
25	Up	hsa05203	Viral carcinogenesis	0.067164	201/7847	0.007343	0.007343	0.051841	9
26	Up	hsa04916	Melanogenesis	0.044776	101/7847	0.007471	0.007471	0.051841	6
27	Up	hsa04976	Bile secretion	0.037313	72/7847	0.007555	0.007555	0.051841	5
28	Up	hsa04971	Gastric acid secretion	0.037313	75/7847	0.00895	0.00895	0.059028	5
29	Up	hsa05220	Chronic myeloid leukemia	0.037313	76/7847	0.009452	0.009452	0.059028	5
30	Up	hsa05418	Fluid shear stress and atherosclerosis	0.052239	139/7847	0.009558	0.009558	0.059028	7
31	Down	hsa04610	Complement and coagulation cascades	0.093023	79/7847	2.07E-06	2.07E-06	0.000341	8
32	Down	hsa05150	Staphylococcus aureus infection	0.069767	68/7847	9.24E-05	9.24E-05	0.007583	6
37	Down	hsa05152	Tuberculosis	0.081395	179/7847	0.003372	0.003372	0.079104	7

gy of HF have been validated by abundant literature in larger patient groups [48–50]. We found herein that miRNA-147a could be an interacted miRNA for HF prediction. According to a previous study [51], miRNA-147a was involved in the macrophage activation during the pathogenesis process of isch-

aemia heart disease; therefore, the cardiac-related miR-147a is somehow consistent with our obtained results. For miR-671-5p, Wong *et al.* [52] recently identified that miR-671-5p and another 7 miRNAs could distinguish HF from healthy controls, which is consistent with our study. However, there is no

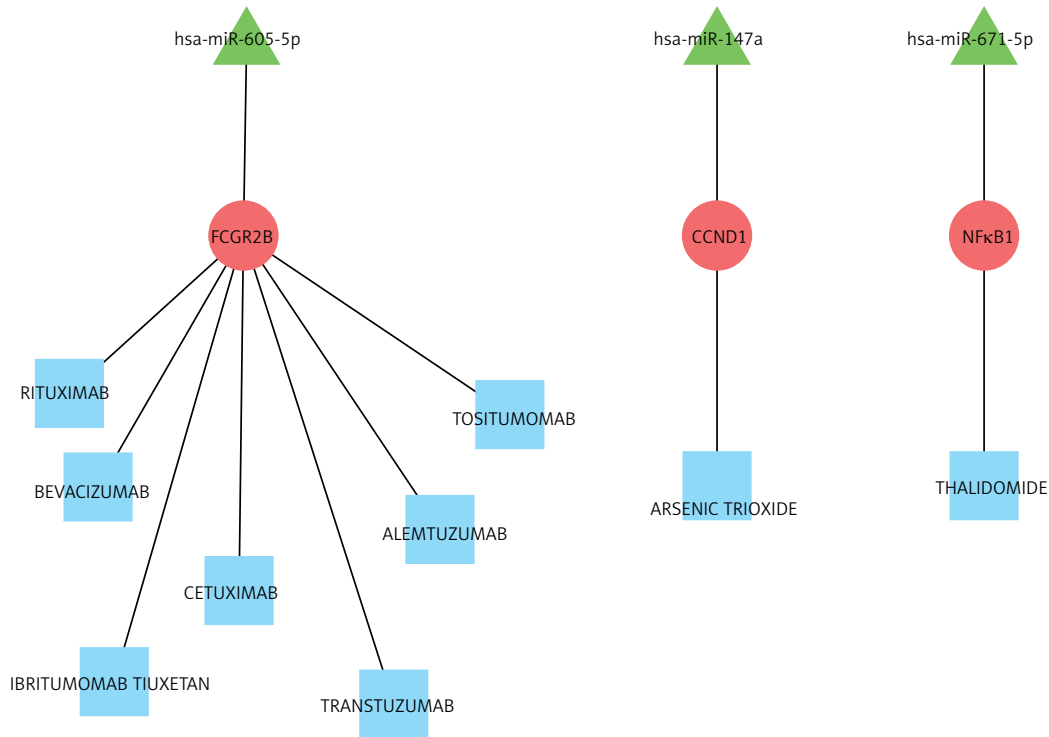


Figure 6. Drug-Gene-miRNA Relationship Network. The green triangle represents the miRNA, the red dot represents the gene, and the blue square represents the drug

report on the role of miRNA-605-5p on the HF, which gave us a new enlightenment for HF study.

In conclusion, taken together, our results indicated that hub genes GAPDH, GALM1, MMP9, CCL5, and GNAL2 were significantly increased in HF. miRNA-605-5p, miRNA-147a, and miRNA-671-5p were predicted as the drug target-interacted gene-miRNA of HF.

Conflict of interest

The authors declare no conflict of interest.

References

1. Centre NCG. Chronic Heart Failure: National Clinical Guideline for Diagnosis and Management in Primary and Secondary Care: Partial Update. 2010.
2. Ponikowski P, Voors AA, Anker SD, et al. 2016 ESC Guidelines for the diagnosis and treatment of acute and chronic heart failure: the task force for the diagnosis and treatment of acute and chronic heart failure of the European Society of Cardiology (ESC). Developed with the special contribution of the Heart Failure Association (HFA) of the ESC. *Eur Heart J* 2016; 18: 891-975.
3. Vos T, Barber RM, Bell B, et al. Global, regional, and national incidence, prevalence, and years lived with disability for 301 acute and chronic diseases and injuries in 188 countries, 1990–2013: a systematic analysis for the Global Burden of Disease Study 2013. *Lancet* 2015; 386: 743-800.
4. Bielecka-Dabrowa A, von Haehling S, Rysz J, Banach M. Novel drugs for heart rate control in heart failure. *Heart Fail Rev* 2018; 23: 517-25.
5. Beiert T, Straesser S, Malotki R, Stöckigt F, Schrickel JW, Andrié RP. Increased mortality and ICD therapies in ischemic versus non-ischemic dilated cardiomyopathy patients with cardiac resynchronization having survived until first device replacement. *Arch Med Sci* 2019; 15: 845.
6. Zeng H, Zheng R, Zhang S, et al. Esophageal cancer statistics in China, 2011: estimates based on 177 cancer registries. *Thorac Cancer* 2016; 7: 232-7.
7. Oka T, Akazawa H, Naito AT, Komuro I. Angiogenesis and cardiac hypertrophy: maintenance of cardiac function and causative roles in heart failure. *Circ Res* 2014; 114: 565-71.
8. Kemi OJ, Ceci M, Wisloff U, et al. Activation or inactivation of cardiac Akt/mTOR signaling diverges physiological from pathological hypertrophy. *J Cell Physiol* 2010; 214: 316-21.
9. Friehs I, Barillas R, Vasilyev NV, Roy N, McGowan FX, del Nido PJ. Vascular endothelial growth factor prevents apoptosis and preserves contractile function in hypertrophied infant heart. *Circulation* 2006; 114: I290.
10. Sun RR, Lu L, Liu M, et al. Biomarkers and heart disease. *Eur Rev Med Pharmacol Sci* 2014; 18: 2927-35.
11. Michalska-Kasiczak M, Bielecka-Dabrowa A, von Haehling S, Anker SD, Rysz J, Banach M. Biomarkers, myocardial fibrosis and co-morbidities in heart failure with preserved ejection fraction: an overview. *Arch Med Sci* 2018; 14: 890.
12. Kadri AN, Kaw R, Al-Khadra Y, et al. The role of B-type natriuretic peptide in diagnosing acute decompensated heart failure in chronic kidney disease patients. *Arch Med Sci* 2018; 14: 1003.
13. Bielecka-Dabrowa A, Sakowicz A, Misztal M, et al. Differences in biochemical and genetic biomarkers in patients with heart failure of various etiologies. *Inter J Cardiol* 2016; 221: 1073-80.

14. Bielecka-Dabrowa A, Sakowicz A, Pietrucha T, et al. The profile of selected single nucleotide polymorphisms in patients with hypertension and heart failure with preserved and mid-range ejection fraction. *Sci Rep* 2017; 7: 8974.
15. Kumarswamy R, Thum T. Non-coding RNAs in cardiac remodeling and heart failure. *Circ Res* 2013; 113: 676-89.
16. Kim EH, Galchev VI, Kim JY, et al. Differential protein expression and basal lamina remodeling in human heart failure. *Proteomics Clin Appl* 2016; 10: 585-96.
17. Smyth GK. *limma: Linear Models for Microarray Data*. Bioinformatics & Computational Biology Solutions Using R & Bioconductor, Springer 2005: 397-420.
18. Boateng HA. Mesh-free hierarchical clustering methods for fast evaluation of electrostatic interactions of point multipoles. *J Chem Phys* 2017; 147: 164104.
19. Sturn A, Quackenbush J, Trajanoski Z. Genesis: cluster analysis of microarray data. *Bioinform* 2002; 18: 207-8.
20. Kanehisa M, Goto S. KEGG: Kyoto Encyclopedia of genes and genomes. *Nucleic Acids Res* 2000; 27: 29-34.
21. Consortium TGO, Ashburner M, Ball CA et al. Gene Ontology: tool for the unification of biology. *Nature Genetics* 2000; 25: 25-9.
22. Szklarczyk D, Franceschini A, Wyder S, et al. STRING v10: protein-protein interaction networks, integrated over the tree of life. *Nucleic Acids Res* 2015; 43: D447.
23. Tang Y, Li M, Wang J, Pan Y, Wu FX. CytoNCA: a cytoscape plugin for centrality analysis and evaluation of protein interaction networks. *Biosystems* 2015; 127: 67-72.
24. Xiong He JZ. Why do hubs tend to be essential in protein networks? *PLOS Genetics* 2006; 2: e88.
25. Bader GD, Hogue CW. An automated method for finding molecular complexes in large protein interaction networks. *BMC Bioinformatics* 2003; 4: 2.
26. Mei Y, You Y, Xia J, Gong JP, Wang YB. Identifying differentially expressed microRNAs between cirrhotic and non-cirrhotic hepatocellular carcinoma and exploring their functions using bioinformatic analysis. *Cell Physiol Biochem* 2018; 48: 1443-56.
27. Liu Y, Hua T, Chi S, Wang H. Identification of key pathways and genes in endometrial cancer using bioinformatics analyses. *Oncol Lett* 2019; 17: 897-906.
28. Dweep H, Gretz N. miRWalk2.0: a comprehensive atlas of microRNA-target interactions. *Nature Methods* 2015; 12: 697.
29. Cotto KC, Wagner AH, Feng YY, et al. DGIdb 3.0: a redesign and expansion of the drug-gene interaction database. *Nucleic Acids Res* 2018; 46: D1068-D1073.
30. Greco S, Fasanaro P, Castelvich S, et al. MicroRNA dysregulation in diabetic ischemic heart failure patients. *Diabetes* 2012; 61: 1633-41.
31. Yang KC, Yamada KA, Patel AY, et al. Deep RNA sequencing reveals dynamic regulation of myocardial noncoding RNAs in failing human heart and remodeling with mechanical circulatory support. *Circulation* 2014; 129: 1009-21.
32. Hu X, Shen G, Lu X, Ding G, Shen L. Identification of key proteins and lncRNAs in hypertrophic cardiomyopathy by integrated network analysis. *Arch Med Sci* 2019; 15: 484.
33. Halade GV, Jin YF, Lindsey ML. Matrix metalloproteinase (MMP)-9: a proximal biomarker for cardiac remodeling and a distal biomarker for inflammation. *Pharmacol Ther* 2013; 139: 32-40.
34. Moshal KS, Rodriguez WE, Sen U, Tyagi SC. Targeted deletion of MMP-9 attenuates myocardial contractile dysfunction in heart failure. *Physiol Res* 2008; 57: 379-84.
35. Wagner DR, Delagardelle C, Ernens I, Rouy D, Vaillant M, Beissel J. Matrix metalloproteinase-9 is a marker of heart failure after acute myocardial infarction. *J Card Fail* 2006; 12: 66-72.
36. Montecucco F, Brauner-Reuther V, Lenglet S, et al. CC chemokine CCL5 plays a central role impacting infarct size and post-infarction heart failure in mice. *Eur Heart J* 2012; 33: 1964.
37. Wang C, Yang H, Gao C. Potential biomarkers for heart failure. *J Cell Physiol* 2019; 234: 9467-74.
38. Seeland U, Selejan S, Engelhardt S, Mä-Ller P, Lohse MJ, Bähr M. Interstitial remodeling in beta1-adrenergic receptor transgenic mice. *Basic Res Card* 2007; 102: 183-93.
39. Vinet L, Rouet-Benzineb P, Marniquet X, et al. Chronic doxycycline exposure accelerates left ventricular hypertrophy and progression to heart failure in mice after thoracic aorta constriction. *Am J Physiol Heart Circ Physiol* 2008; 295: H352-60.
40. Brattelid T, Winer LH, Levy FO. Reference gene alternatives to Gapdh in rodent and human heart failure gene expression studies. *BMC Mol Biol* 2010; 11: 1-10.
41. Zhang T, Brown JH. Role of Ca²⁺/calmodulin-dependent protein kinase II in cardiac hypertrophy and heart failure. *Cardiovasc Res* 2004; 63: 476-86.
42. Liu Z, Liu X, Yu H, et al. Common variants in TRDN and CALM1 are associated with risk of sudden cardiac death in chronic heart failure patients in Chinese Han population. *PLoS One* 2015; 10: e0132459.
43. Marsman RF, Barc JG, Beekman L, Bhuijan ZA, Wilde AAM, Bezzina CR. A mutation in CALM1 encoding calmodulin causes sudden cardiac death in childhood and adolescence. *Eur Heart J* 2013; 34: P2298-P2298.
44. Vegter EL, Peter VDM, De Windt LJ, Pinto YM, Voors AA. MicroRNAs in heart failure: from biomarker to target for therapy. *Eur J Heart Fail* 2016; 18: 457-68.
45. Melman YF, Shah R, Das S. MicroRNAs in heart failure: is the picture becoming less miRky? *Circ Heart Fail* 2014; 7: 203-14.
46. Bagnall RD, Tsoutsman T, Shephard RE, Ritchie W, Semarian C. Global MicroRNA profiling of the mouse ventricles during development of severe hypertrophic cardiomyopathy and heart failure. *PLOS One* 2012; 7: e44744.
47. Tijssen AJ, Creemers EE, Moerland PD, et al. MiR423-5p as a circulating biomarker for heart failure. *Circ Res* 2010; 106: 1035-39.
48. Ikeda S, Kong SW, Lu J, et al. Altered microRNA expression in human heart disease. *Physiol Genomics* 2007; 31: 367-73.
49. Dirx E, Da CMP, De Windt LJ. Regulation of fetal gene expression in heart failure. *Biochim Biophys Acta* 2013; 1832: 2414-24.
50. Ellis KL, Cameron VA, Troughton RW, Frampton CM, Ellmers LJ, Richards AM. Circulating microRNAs as candidate markers to distinguish heart failure in breathless patients. *Eur J Heart Fail* 2013; 15: 1138-47.
51. Liu G, Friggeri A, Yang Y, Park YJ, Tsuruta Y, Abraham E. miR-147, a microRNA that is induced upon Toll-like receptor stimulation, regulates murine macrophage inflammatory responses. *Proc Natl Acad Sci USA* 2009; 106: 15819-24.
52. Wong LL, Armugam A, Sepramaniam S, et al. Circulating microRNAs in heart failure with reduced and preserved left ventricular ejection fraction. *Eur J Heart Fail* 2015; 17: 393-404.